40 (1995).
31. F. Croce, S. D. Brown, S. G. Greenbaum, S. M. Slane, and M. Salomon, *Chem. Mater.*, **5**, 1268 (1993).
32. H. S. Choe, B. G. Carroll, D. M. Pasquariello, and K. M. Abraham, *ibid.*, **17**, 369 (1997).
33. Y. Kato, M. Watanabe, K. Saui, and N. Ogata, *Solid State Ionics*, **40/41**, 632 (1990).
34. Z. Bashir, *Polymer*, **33**, 4304 (1992).
35. G. J. Janz, J. Ambrose, J. W. Coutts, and J. R. Downey, Jr., *Spectrochim. Acta*, **35A**, 175 (1979).
36. G. Fini, P. Mirone, and B. Fortunato, *J. Chem. Soc., Faraday Trans. 2*, **69**, 1243 (1973).
37. Z. Deng and D. E. Irish, *J. Chem. Soc., Faraday Trans.*, **88**, 2891 (1992).
38. S. Hydo and K. Okabayashi, *Electrochim. Acta*, **34**, 1551 (1989).
39. S. Hyodo, K. Oyabayashi, and A. Yoshida, *Prep. Denchi Touronkai Jpn.*, 3B05, 195 (1989).
40. U. Olsher, R. M. Izatt, J. S. Bradshaw, and N. K. Dalley, *Chem. Rev.*, **91**, 137 (1991) and references therein.

Synthesis of $LiCoO_2$ by Decomposition and Intercalation of Hydroxides

Yet-Ming Chiang,* Young-Il Jang, Haifeng Wang, Biying Huang, Donald R. Sadoway,* and Peixiang Ye**

Department of Materials Science and Engineering, Massachusetts Institute of Technology, Cambridge, Massachusetts 02139, USA

ABSTRACT

A low-temperature, solid-state process for the synthesis of high-quality intercalation oxides has been developed. Finely divided cobalt hydroxide–lithium hydroxide mixtures, prepared by precipitation and freeze-drying, transform directly to highly ordered $LiCoO_2$ of the α-$NaFeO_2$ structure type (high-temperature $LiCoO_2$) upon firing in air at temperatures of 200–300 °C. The mechanism of transformation has been determined using transmission electron microscopy and X-ray diffraction. Crystallites of $Co(OH)_2$ decompose and intercalate with Li to form $LiCoO_2$ without changing particle shape, orientation, or crystallinity. The absence of a CoOOH intermediate phase indicates that the intercalation step is rapid compared to the $Co(OH)_2 \rightarrow$ CoOOH decomposition. Although the product obtained at temperatures as low as 100 °C is electrochemically active, firing at higher temperatures further improves capacity and cyclability.

Introduction

Intercalation compounds of the layered rocksalt structure such as $LiCoO_2$ and $LiNiO_2$, and spinels such as $LiMn_2O_4$, are widely studied and used as electrodes in advanced lithium batteries.[1-4] The composition, structure, and cation ordering of these compounds determine the intercalation voltage[5,6] and theoretical charge capacity, whereas extrinsic factors such as particle size and microstructure have important influence on characteristics such as cycle life and power capability. A wide variety of methods has been employed in the synthesis of intercalation oxides.[7-12] Reactions using lithium carbonate or lithium hydroxide and various transition metal salts are the most widely practiced. A typical "solid-state reaction" process involves firing the metal salt mixtures at 900–1000 °C for >24 h, sometimes with intermediate grindings, in order to achieve homogeneity. When Li_2CO_3 is used, the reaction may involve molten carbonate because the firing temperatures lie above its melting point (723 °C). In the most widely studied compound, $LiCoO_2$, high-temperature firing for many hours is necessary to obtain the α-$NaFeO_2$ cation ordering (so-called HT $LiCoO_2$)[10,13] when starting with physically mixed metal salts. Lower temperature firing has been observed to result in the "low-temperature (LT $LiCoO_2$)" structure, which is a partially disordered rocksalt solid solution with inferior electrochemical performance.[10,13]

The fact that lithium intercalation oxides exhibit high mobility at room temperature for not only Li^+ but also H^+ suggests that the intercalation of hydroxides can be a synthesis approach. Amatucci et al.[7] have used a hydrothermal method to synthesize $LiCoO_2$ and $LiNiO_2$ from CoOOH and NiOOH precursors, recognizing that the oxyhydroxide is isomorphous with the oxide, differing primarily in the substitution of H^+ ions for Li^+. They first decomposed $Co(OH)_2$ to CoOOH and then equilibrated the oxyhydroxide with highly basic lithium hydroxide solution in an autoclave to promote liquid-phase ion exchange between H^+ and Li^+, thereby obtaining well-ordered HT $LiCoO_2$. Larcher et al.[12] have studied the hydrothermal synthesis in additional detail.

We reasoned that because these transition-metal hydroxides, as well as lithium hydroxide, are unstable with respect to their oxides at modest temperatures in gaseous ambients of low water activity, hydrothermal synthesis should not be necessary to effect the same kind of Li^+–H^+ ion exchange. If the hydroxide could be decomposed in the presence of a lithium source, then the layered rocksalt structure might form directly through Li^+ intercalation. Crystallization of the LT phase or other intermediate phases (e.g., Co_3O_4 [10]) might thereby be avoided. Compared to other solid-state precursors, hydroxide precursors yield only water as the decomposition product, giving a much "cleaner" decomposition than is possible with metallorganic precursors such as acetates[8] or citrates (the Pechini process).[9] The latter process in particular produces large amounts of volatile organics upon pyrolysis.

The results in this paper show that homogeneously dispersed hydroxide precursors can be decomposed and intercalated in the solid state at temperatures as low as 100 °C, with highly ordered $LiCoO_2$ being obtained by 200–300 °C. Transmission electron microscopy (TEM) and X-ray diffraction (XRD) have clarified the mechanism by which this occurs.

Precipitation and Freeze-Drying

In order to obtain a homogenous and finely dispersed mixture of the hydroxides, we freeze-dried a suspension of $Co(OH)_2$ in aqueous lithium hydroxide solution. A suspension was necessary because all well-known Li salts are soluble in water and cannot be precipitated in the same pH range at which $Co(OH)_2$ is insoluble.[15] $Co(OH)_2$ was precipitated by adding a 0.1 M solution of $Co(NO_3)_2$ (Johnson Matthey Catalog Company, 99.5%) in deionized water to a stirred aqueous solution of $LiOH \cdot H_2O$ in deionized water, continuously monitored and titrated to maintain the pH at 11, near the minimum solubility point for $Co(OH)_2$. [15] After precipitation the suspension was equilibrated at room temperature without stirring for 12 h and then settled by centrifugation. A critical step was the removal of nitrate ions

* Electrochemical Society Active Member.
** Electrochemical Society Student Member.

from the suspension, which otherwise form low-melting nitrate compounds upon drying. Upon subsequent firing, melting of these salts can cause compositional segregation. The supernatant liquid from the precipitation was first decanted, and the $Co(OH)_2$ ultrasonically dispersed in a buffer solution of $LiOH{\cdot}H_2O$ in water at pH 11. The precipitate was settled by centrifugation and the supernatant again decanted. For complete rinsing, this cycle of dispersion in buffer solution, settling by centrifugation, and decanting was conducted a total of five times. Because the precipitation and rinsing are conducted at room temperature, the amount of Li^+–H^+ exchange between the hydroxide and the LiOH solution is likely insignificant. This is clear upon comparing the present synthesis conditions with the temperatures and pressures necessary to achieve ion exchange in hydrothermal experiments.[7,12]

To obtain a highly homogeneous physical mixture of LiOH and $Co(OH)_2$, the rinsed precipitate was dispersed a final time in an aqueous solution containing dissolved $LiOH{\cdot}H_2O$ at a concentration sufficient to yield an overall composition with a 1:1 Li:Co ratio, asssuming there was no prior Li ion exchange with the hydroxide during the synthesis. This suspension was then atomized into liquid nitrogen and the frozen droplets freeze-dried (Consol 12LL, The Virtis Company, Gardiner, NY) to obtain a uniform and fine dispersion of crystalline $Co(OH)_2$ and LiOH (partially hydrated). Figure 1 shows the microstructure of this precursor. Hexagonal platelets of $Co(OH)_2$ are observed of 0.2–0.5 μm diam. The thickness was typically 1/10 the platelet width. The freeze-dried lithium hydroxide formed a lacy solid surrounding each platelet and is amorphous by XRD.

To compare the decomposition characteristics of this carefully prepared, highly homogeneous precursor with a simpler preparation of the same components, limited experiments were also conducted[16] using commercially available $Co(OH)_2$ and $LiOH{\cdot}H_2O$, which were mixed by ball-milling in a polypropylene container using alumina milling media and then calcined in air.

Decomposition and Intercalation

Figure 2 shows XRD scans of the powder for isochronal firings (2 h) in air at temperatures ranging from 100 to 600 °C. The precursor contains $Co(OH)_2$ as the predominant crystalline phase, with minor amounts of Li_2CO_3 and possibly some $CoOOH/LiCoO_2$. The trace Li_2CO_3 results from exposure to residual CO_2 in the air; conducting the synthesis in CO_2-free ambient reduced the amount of this phase to below X-ray detection limits. The LiOH phase was not detectable in the XRD pattern but was determined by TEM to be amorphous. Upon firing at 100 °C for 2 h the strongest lines for $Co(OH)_2$ [(100), (101), and (102)] are greatly diminished, whereas those for $LiCoO_2$ appear. With increasing firing temperature, the residual Li_2CO_3 disappears and increasingly sharper lines appear with position and relative intensities indicating single-phase well-crystallized HT $LiCoO_2$. Gummow et al.[13] have discussed the structural distinctions between LT $LiCoO_2$ and HT $LiCoO_2$. In powder XRD, HT $LiCoO_2$ is distinguished by the high intensity of the (003) line and clear splitting between the (006)/(012) and (108)/(110) lines. In Fig. 2, all these features are clearly evident in samples fired at 300 °C and above. Some peak broadening does remain up to 500 °C. CoOOH and $LiCoO_2$ are distinguishable from one another by the relative intensities of the (101)/(012) and (104)/(015) lines.[14] In Fig. 2, where the peak positions for CoOOH are labeled, the relative intensities of these lines indicate that it is $LiCoO_2$ and not CoOOH which is the predominant phase, although some solid solution of the two cannot be ruled out at the lowest calcining temperatures (100 and 200 °C).

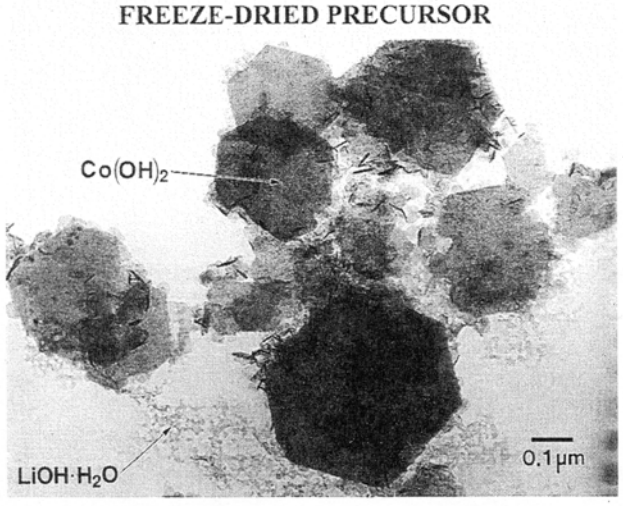

Fig. 1. Precipitated and freeze-dried mixture of cobalt hydroxide and lithium hydroxide, showing hexagonal plate morphology of the former, finely dispersed with the latter.

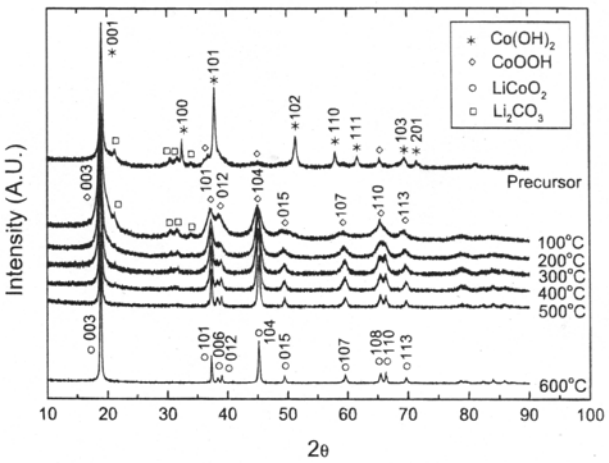

Fig. 2. Powder XRD scans for the precursor shown in Fig. 1 and after calcining for 2 h in air at the indicated temperature. Although CoOOH and $LiCoO_2$ share closely similar peak positions, the relative intensities of the (006)/(012) and (108)/(110) peaks distinguish the phase obtained, even after firing at only 100 °C, as $LiCoO_2$.[13]

TEM observations of the powders at various stages of calcining (corresponding to the XRD results in Fig. 2) are shown in Fig. 3 and 4. Selected-area electron diffraction (Fig. 3a) showed that each hexagonal platelet of $Co(OH)_2$ (space group $P\bar{3}m1$, $a_o = 0.3183$ nm, $c_o = 0.4652$ nm) in the precursor is a single crystal, with the platelet face being normal to [0001] and the plate edges normal to [$10\bar{1}0$]. This single-crystallite morphology was preserved throughout the transformation to $LiCoO_2$. After calcining at 100 °C for 2 h, (Fig. 3b), the platelet remains single crystalline, while XRD (Fig. 2) shows that $Co(OH)_2$ has largely transformed to $LiCoO_2$. Upon firing at 300 °C, all the lithium salt disappeared from the TEM image (Fig. 3c). The same is observed in samples fired at 400 and 500 °C (Fig. 3d and e), indicating that only the $LiCoO_2$ phase is present. Notice that each particle remains throughout an oriented single crystal, the platelet normal now being [0001] of the $LiCoO_2$ structure (space group $R\bar{3}m$, $a_o = 0.2816$ nm, $c_o = 1.4051$ nm in the hexagonal setting). No evidence for nucleation of new $LiCoO_2$ phase particles is seen in any of the samples. These results show that $Co(OH)_2$ transforms to $LiCoO_2$ by Li^+ intercalation, which for charge neutrality must be accompanied by H^+ diffusion outward.

Figure 3a-e also shows a striking mosaic submicrostructure appearing within each particle during the transformation to $LiCoO_2$. This may result from local stresses forming upon substituting Li^+ for H^+. The submicrostructure, initially of nanometer scale, coarsens systematically with increasing temperature. Throughout, electron diffraction

shows that each particle remains a single crystal. The sharpness of the reflections indicate that the mosaic submicrostructure giving diffraction contrast in the bright-field image results primarily from tilts of the subgrains rather than from significant rotational misorientations. With increasing firing temperature, the size of the subgrains increases systematically. The platelet shape of the particles is retained until about 600 °C, (Fig. 4), when the particles begin to spheroidize and the mosaic submicrostructure largely disappears. After firing at 800 °C for 2 h, individual grains are equiaxed and have an average diameter of ~0.3 μm, but the grains are sintered into larger aggregates (Fig. 5).

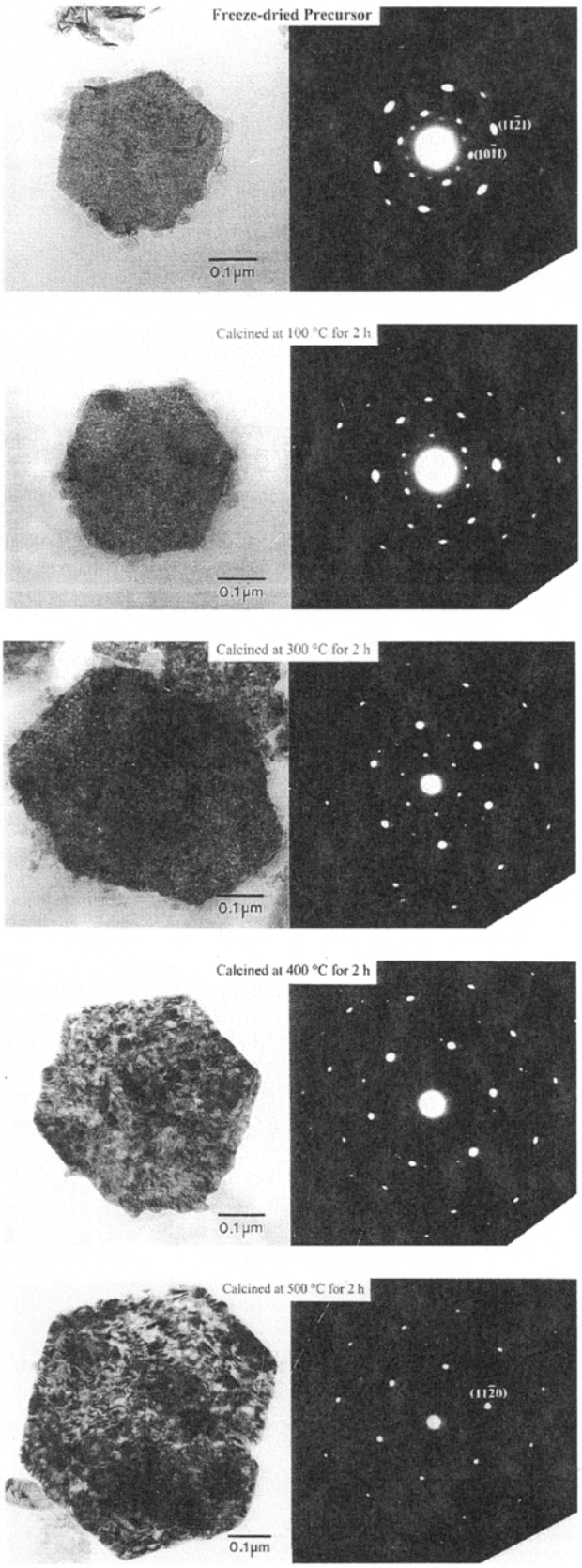

Fig. 3. Bright-field TEM image, and corresponding selected area electron diffraction pattern, of (a) the hydroxide precursor, and after firing for 2 h in air at (b) 100, (c) 300, (d) 400, and (e) 500 °C. Notice that the morphology and single crystallinity of the particles is maintained. A submicrostructure of misoriented domains of nanometer-length scale develops and coarsens within the crystallites.

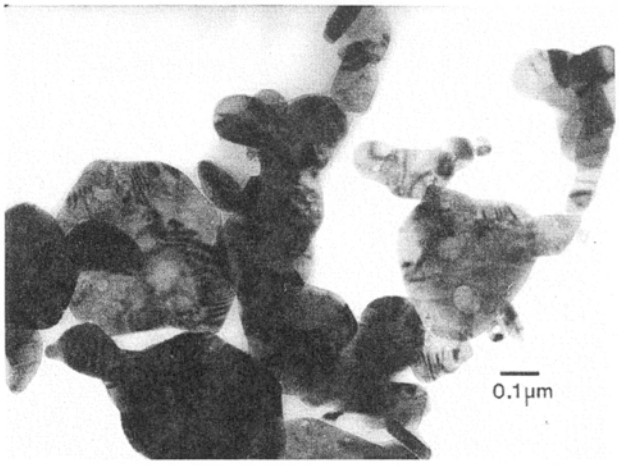

Fig. 4. After firing at 600 °C in air for 2 h, the hexagonal platelet crystallites have begun to spheroidize.

The specific surface areas of the powders, as measured by the Brunauer–Emmett–Teller (BET) method, remains relatively constant until firing temperatures at which particle coarsening is also seen by TEM are reached. As shown in Fig. 6, the specific surface area is 22–24 m^2/g for the precursor and for samples fired below 400 °C but decreases sharply with increasing firing temperature above that temperature. If it is assumed that the particles have the bulk density of $LiCoO_2$ (5.08 g/cm^3), the measured specific surface areas are consistent with dense particles of the average platelet size and aspect ratio observed by TEM. That is, the mosaic domains of the platelets are a submicrostructure of a dense particle, rather than being free-standing nanoparticles.

CoOOH (space group $R\bar{3}m$, a_o = 0.2855 nm, c_o = 1.3156 nm) is conceptually a likely intermediate in the

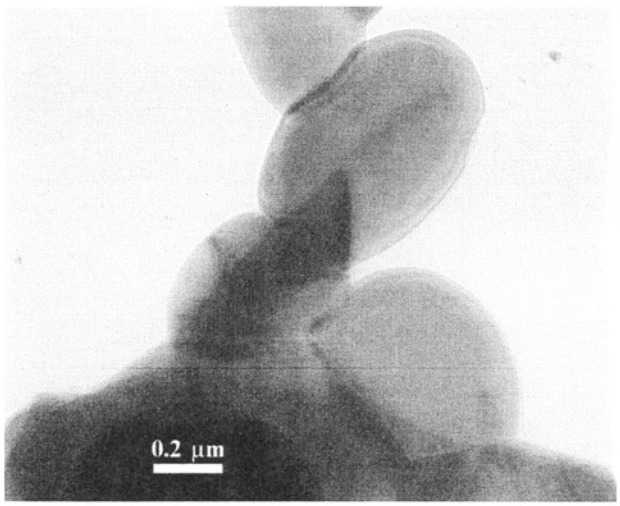

Fig. 5. Firing at 800 °C in air for 2 h yields equiaxed primary particles in a sintered aggregate morphology.

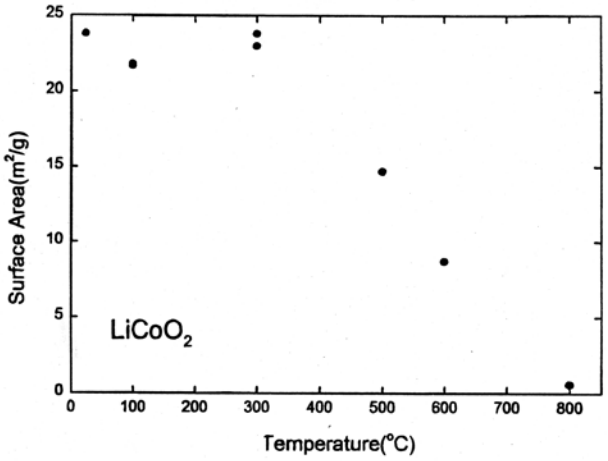

Fig. 6. BET surface area measurements for powders fired for 2 h in air at various temperatures show that the specific surface area remains relatively constant below 400 °C but decreases at higher firing temperatures, where TEM correspondingly shows coarsening and spheroidization of the powder particles.

transformation, being the product of $Co(OH)_2$ decomposition and being isostructural with $LiCoO_2$. The decomposition and intercalation steps can be written as the separate reactions

$$2Co(OH)_2 + \frac{1}{2}O_2(g) \rightarrow 2CoOOH + H_2O \quad [1]$$

$$CoOOH + LiOH{\cdot}H_2O \rightarrow LiCoO_2 + 2H_2O(g) \quad [2]$$

The hydrothermal synthesis of Amatucci et al.[7] used reaction 2. In the present experiments, both reactions occur in sequence. The absence of a clearly distinguishable CoOOH intermediate indicates that 2 occurs rapidly and is not the rate-limiting step for the overall transformation.

The experiments conducted using simple physical mixtures (ballmilled) of $Co(OH)_2$ and $LiOH{\cdot}H_2O$ showed conversion to HT $LiCoO_2$ upon calcining at 600 °C for 2 h or more. Results from a sample fired at 600 °C for 8 h, Fig. 7, show well-ordered HT $LiCoO_2$. This can be compared with the firing temperatures of T > 900 °C and times of >24 h necessary to obtain single-phase material in conventional processing with oxide and carbonate precursors.

It is interesting that Garcia et al.[10,11] also made $LiCoO_2$ by precipitating $Co(OH)_2$ from aqueous solutions of $Co(NO_3)_2$ using LiOH, yet they obtained very different results. Instead of obtaining the HT structure directly as we do, they obtained LT $LiCoO_2$. The difference in phase evolution between their experiments and ours can be traced to the fact that they did not remove nitrate species from the precipitated material; they instead dried the precipitate and the solution together. Thus, upon firing, they report decomposition of ammonium nitrate at 212 °C followed by melting of $LiNO_3$ at 264 °C, leaving Co_3O_4 as the Co-rich phase. At 400 °C, LT $LiCoO_2$ subsequently crystallizes. In the present process, removal of the nitrate ions from the precipitated $Co(OH)_2$ suspension allows the hydroxide crystallites to be preserved and to act as templates from which HT $LiCoO_2$ crystallizes.

Electrochemical testing.—The powders prepared by the new precipitation/freeze-drying method were electrochemically tested. Composite cathodes were fabricated in which the oxide powder was combined with graphite and poly(vinylidene) difluoride (PVDF) as a binder and tested in a coin cell against Li metal anodes using 1 M $LiPF_6$ in ethylene carbonate–diethylene carbonate as the electrolyte. The first charge/discharge cycle for powders calcined at 100, 300, 600, and 800 °C, using a current density of 0.4 mA/cm² and voltage limits of 4.25–2.5 V, is shown in Fig. 8. Although the charging curves for all four powders are similar, the first-discharge capacity increased significantly as the firing temperature increased, being 91, 106, 116, and 140 mAh/g for the four respective calcining temperatures. Cycling tests were also conducted on some samples over a range of current densities. The charge and discharge capacities for three samples, cycled between 2.5 and 4.25 V, are plotted vs against cycle number in Fig. 9. The sample calcined at 100 °C shows rapid capacity fade at a current density of 0.4 mA/cm². However, the samples calcined at 600 and 800 °C showed good resistance to capacity fade, both at 0.4 mA/cm² (not shown) and at higher current densities of 1.2 and 0.8 mA/cm², respectively, shown in Fig. 9. More detailed electrochemical tests of these materials will be reported elsewhere.

Comparing the samples fired at 100 and 300 °C, the latter has much improved capacity despite a similar BET surface area (Fig. 6), which may be related to more complete decomposition and intercalation. For the samples fired at higher temperatures, we continue to see a trend of increasing capacity with decreasing specific surface area, as has also been reported by others.[12] These differences may not be intrinsic to the powders. TEM (Fig. 3–5) and XRD (Fig. 2) shows that the powders fired at or above 300 °C are well-crystallized as the α-$NaFeO_2$ structure. Our tests, like most, use a three-phase composite cathode flooded with electrolyte in which the electrolyte provides ionic conductivity and the carbon phase provides electronic conductivity. Since the powder with the highest capacity and best cycle life (fired at 800 °C) is also the most aggregated (Fig. 5), it may be that the coarser powder aggregates simply allow a

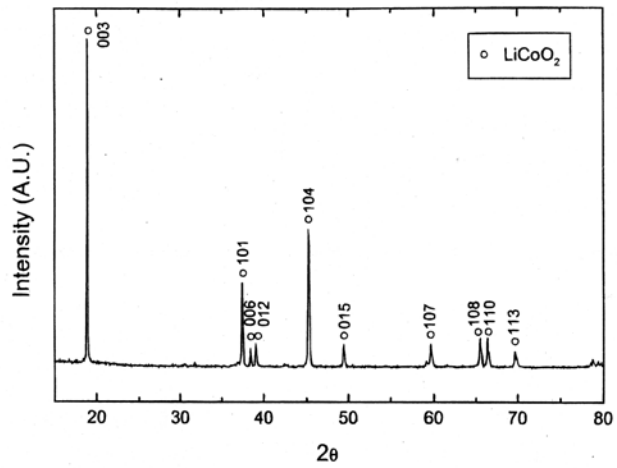

Fig. 7. Powder XRD scan for a $LiCoO_2$ sample prepared by ballmilling $Co(OH)_2$ and $LiOH{\cdot}H_2O$ powders and firing at 600 °C for 8 h.

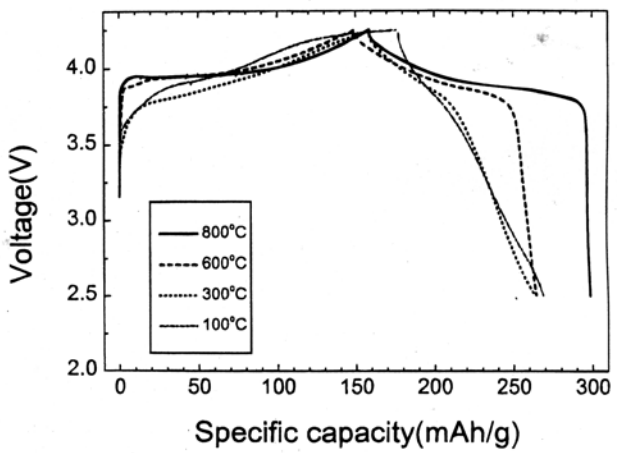

Fig. 8. First charge-discharge curves for powders calcined 2 h in air at the indicated temperature and tested against a Li metal anode in a coin cell at 0.4 mA/cm² current density.

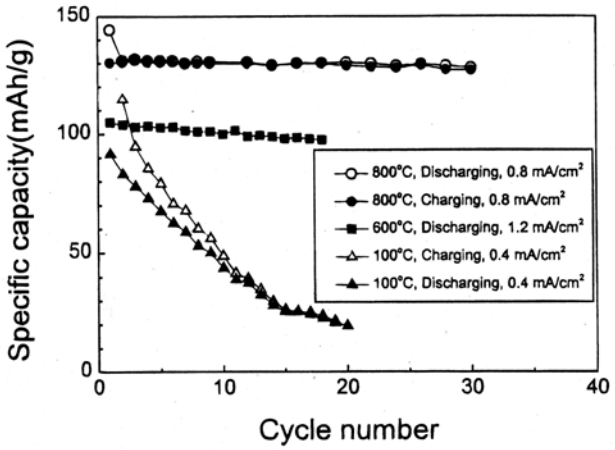

Fig. 9. Specific capacity vs cycle number for selected powders cycled between 2.5 and 4.25 V tested at the indicated current densities.

greater fraction of the powder to be electrochemically accessed. The powders calcined at lower temperature may have equivalent intrinsic performance but are not fully used in the present composite structures. Further study is necessary to confirm whether this is the case.

Conclusions

A synthesis method using finely divided $Co(OH)_2$ and LiOH precursors is shown to yield $LiCoO_2$ of well-ordered α-$NaFeO_2$ structure upon firing in air at temperatures as low as 200–300 °C. TEM and XRD observations show that the $Co(OH)_2$ precursor decomposes and intercalates Li to form $LiCoO_2$ while retaining the crystal structure and particle morphology of the parent hydroxide. Firing of simple physical mixtures of the hydroxides also results in synthesis of well-ordered $LiCoO_2$ at reduced temperatures and times compared to conventional solid-state reactions. This mechanism allows the low-temperature synthesis of $LiCoO_2$ with excellent electrochemical performance from convenient solid-state hydroxide precursors and may be useful for other intercalation oxides as well.

Acknowledgments

We thank G. Ceder and A. M. Mayes for helpful discussions, M. Lundberg for experimental assistance, and M. Chanda, C. P. Manning, M. T. Platero, and S. L. Wordsworth for the results in Fig. 7. This work was supported by Furukawa Electric Company and the Idaho National Engineering and Environmental Laboratory under Grant no. C95-175002 and used instrumentation in the Shared Central Facilities at MIT supported by NSF Grant no. 9400334-DMR.

Manuscript submitted June 2, 1997; revised manuscript received October 30, 1997.

Massachusetts Institute of Technology assisted in meeting the publication costs of this article.

REFERENCES

1. B. C. H. Steele, in *Fast Ion Transport in Solids*, W. Van Gool, Editor, p. 103, North Holland, Amsterdam (1973).
2. L. Heyne, *ibid.*, p. 123.
3. M. S. Whittingham, *Prog. Solid State Chem.*, **12**, 41 (1978) .
4. S. Megahed and B. Scrosati, *J. Power Sources*, **51**, 79 (1994).
5. G. Ceder, M. K. Aydinol, and A. F. Kohan, *Comput. Mater. Sci.*, **8**, 161 (1997).
6. M. K. Aydinol, A. F. Kohan, G. Ceder, K. Cho, and J. Joannopoulos, *J. Power Sources, Phys. Rev. B*, **56**, 1354 (1997).
7. G. G. Amatucci, J. M. Tarascon, and L. C. Klein, *Solid State Ionics*, **84**, 169 (1996).
8. P. Barboux, J. M. Tarascon, and F. K. Shokoohi, *J. Solid State Chem.*, **94**, 185 (1991).
9. W. Liu, G. C. Farrington, F. Chaput, and B. Dunn, *This Journal*, **143**, 879 (1996).
10. B. Garcia, P. Barboux, F. Ribot, A. Kahn-Harari, L. Mazerolles, and N. Baffier, *Solid State Ionics*, **80**, 111 (1995).
11. B. Garcia, J. Farcy, J.P. Pereira-Ramos, and N. Baffier, *This Journal*, **144**, 1179 (1997).
12. D. Larcher, M. R. Palacin, G. G. Amatucci, and J.-M. Tarascon, *ibid.*, **144**, 408 (1997).
13. R. J. Gummow, M. M. Thackeray, W. I. F. David, and S. Hull, *MRS Bull.*, **27**, 327 (1992).
14. Joint Committee on Powder Diffraction Standards, File no. 44-0145 ($LiCoO_2$) and 7-169 (CoOOH).
15. C. F. Baes, Jr. and R. E. Mesner, *The Hydrolysis of Cations*, John Wiley & Sons, New York (1976).
16. M. Chanda, C. P. Manning, M. T. Platero, and S. L. Wordsworth, Unpublished work.